Stability Analysis of Bipedal Walking with Control or Monitoring of the Center of Pressure

D. Djoudi and C. Chevallereau

IRCCyN, Ecole Centrale de Nantes, Université de Nantes, UMR CNRS 6597
BP 92101, 1 rue de la Noë, 44321 Nantes cedex 3, France
{Dalila.Djoudi,Christine.Chevallereau}@irccyn.ec-nantes.fr

Summary. The objective of this study is to analyze the stability of two control strategies for a planar biped robot. The unexpected rotation of the supporting foot is avoided via the control of the center of pressure or CoP. For the simultaneous control of the joints and of the CoP, the system is under-actuated in the sense that the number of inputs is less than the number of outputs. Thus a control strategy developed for planar robot without actuated ankles can be used in this context. The control law is defined in such a way that only the geometric evolution of the biped configuration is controlled, but not the temporal evolution. The temporal evolution during the geometric tracking is completely defined and can be analyzed through the study of a model with one degree of freedom. Simple conditions, which guarantee the existence of a cyclic motion and the convergence toward this motion, are deduced. These results are illustrated with some simulation results. In the first control strategy, the position of the CoP is tracked precisely, in the second one, only the limits on the CoP position are used to speed-up the convergence to the cyclic motion.

1 Introduction

The control of many walking robots is based on the notion of center of pressure CoP [11, 12] also called ZMP by Vukobratovic and his co-workers [14, 13]. As long as the CoP remains inside the convex hull of the foot-support, the supporting foot does not rotate and the contact with the ground is guaranteed. Control strategies are often decomposed into a low level and a high level. The low level ensures the tracking of the reference motion, and the high level modifies the reference motion in order to ensure that the CoP remains inside the convex hull of the foot-support.

Since the respect of the expected condition of contact with the ground is more important than a tracking error, this kind of control strategy is interesting. In many experimental works, how to modify the reference motion is not

detailed [11], and it seems that this point has not been studied theoretically. The modification of the reference motion has obviously an important effect on the stability of the walking (in the sense of the convergence toward a cyclic motion) and its robustness (in the sense of the reaction of the robot in the presence of perturbation).

Our control strategy is based on simultaneous control of the joint and on the evolution of the CoP position. The unexpected rotation of the supporting foot is avoided via the control of the position of the center of pressure. Since the joints and the position of the CoP are controlled simultaneously, the system becomes under-actuated in the sense that the number of inputs is less than the number of outputs. Thus a control strategy developed for planar robots without actuated ankles can be used in this context [9, 2, 4]. An extension of the work of Westervelt et al. [15], for the completely actuated robot based on a prescribed evolution of the ankle torque was proposed [5]. In the proposed study, the position of the CoP is prescribed, not the ankle torque.

The control law is defined in such a way that only the geometric evolution of the biped configuration is controlled, but not the temporal evolution. This strategy can be seen as an on-line modification of the joint reference motion with respect to time in order to ensure that the position of the center of pressure will be satisfying. The modification of the reference motion corresponds to determine the acceleration along a given path[1] in the joint space. This modification is interesting in the presence of impact, because for all the possible reference motions, the configuration of the robot at impact is the same, and the set of all the reference motions is invariant with respect to impact. As a consequence the impact phase, and the possible variation of the instant of impact have no disturbing effect [3].

Assuming a perfect robot model, and without perturbation, the temporal evolution during the geometric tracking is completely defined and can be analyzed through the study of a model with one degree of freedom. The Poincaré return map can be used to study the stability of the proposed control law.

The practical constraints on the position of the CoP do not imply that this point follows exactly a desired path, but that the position of the CoP evolves between some limits. Thus a second control law is proposed to speed up the convergence to the cyclic motion. The position of the CoP is no longer controlled but only monitored to avoid the rotation of the supporting foot [3]. In this case the control strategy is based on a heuristics proposed by Wieber [16]. In this paper a stability study of this control law is proposed.

Section 2 presents the dynamic model of the biped. A planar biped model with massless feet is considered. Section 3 is devoted to the formulation of the first control strategy and to the existence of a cyclic motion. In Sect. 4 we present the second control strategy. Some simulation results are presented in Sect. 5 in the case of a precise modeling of the robot and in Sect. 6 in the

[1] The time evolution is not specified for a path.

case of an imprecise modeling. Some properties of the two control strategies are given in Sect. 7. Section 8 concludes the paper.

2 Bipedal Model

2.1 The Biped

The biped under study walks in a vertical sagittal xz plane. It is composed of a torso and two identical legs. Each leg consists of two segments and a massless foot. The ankles, the knees and the hips are one-degree-of-freedom rotational frictionless joints. The walk is considered as single support phases separated by impacts (instantaneous double support) with a full contact between the sole of the feet and the ground. The angle of the supporting knee is denoted q_1. The angle of the supporting hip is denoted q_2. The angle of the swing hip is denoted q_3. The angle of the swing knee is denoted q_4. During swing phase the foot is aligned horizontally thus the angle of the swing ankle can be calculated. The supporting ankle angle allows to choose the orientation of the supporting shank with respect to the vertical q_5. Vector $q = [q_1, q_2, q_3, q_4, q_5]^T$ of variables (Fig. 1) describes the shape of the biped during single support. Since the free foot is massless no torque is required at the swing ankle. The torque at the supporting ankle will be treated in a special way thus it is denoted $\Gamma_a = \Gamma_5$. The torques are grouped into a torque vector $\Gamma = [\Gamma_1, \Gamma_2, \Gamma_3, \Gamma_4, \Gamma_5]^T$.

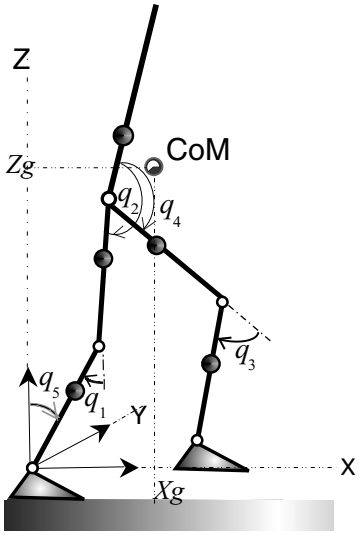

Fig. 1. The studied biped: generalized coordinates

In the simulation, we use the following biped parameters [2]. The lengths of the thighs and of the shanks are 0.4 m. However, their masses are different: 6.8 kg for each thigh and 3.2 kg for each shank. The length of the torso is 0.625 m and its mass is 17.05 kg. The center of mass are placed on the line representing the link in Fig. 1. The distance between the joint actuator and the center of mass is 0.1434 m for the torso, 0.163 m for the shanks, and 0.123 m for the thigh. The moments of inertia of the segments are also taken into account, there values are defined around the joint axis, and there value are 1.8694 kgm^2 for the torso, 0.10 kgm^2 for the shanks, and 0.25 kgm^2 for the thigh. The inertia of the motor of the hip and of the knee are 0.83 kgm^2. The feet is massless and have no inertia. The size of the feet are $h_p = 0.08$ m, $l_{min} = 0.06$ m, $l_{max} = 0.2$ m (Fig. 2).

2.2 Dynamic Modeling

The walking gait is composed of stance phases. A passive impact separates the stance phases. The legs swap their roles from one step to the next one. Thus the study of a step allows us to deduce the complete behavior of the robot. Only a single support phase and an impact model are derived.

The Single Support Phase Model

Using Lagrange's formalism, the i^{th} line of the dynamic model for $i = 1, \ldots, 5$ (q_i is the i^{th} element of vector q) is:

$$\frac{d}{dt}\left(\frac{\partial K}{\partial \dot{q}_i}\right) - \frac{\partial K}{\partial q_i} + \frac{\partial P}{\partial q_i} = Q_i \tag{1}$$

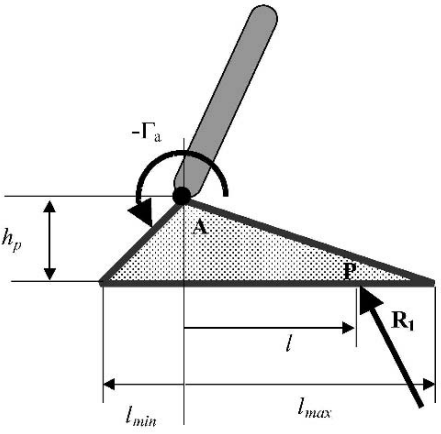

Fig. 2. The equilibrium of the supporting foot

where K is the kinetic energy and P is the potential energy. The virtual work δW of the external torques and forces, given by expression $\delta W = \sum Q_i \delta q_i = Q^T \delta q$, defines the vector Q of the generalized forces.

The kinetic energy K is independent of the coordinate frame chosen. Since coordinate q_5 defines the orientation of the biped as a rigid body, the inertia matrix is independent of this variable, it depends only of "internal" variables represented by vector $q_c = [q_1, q_2, q_3, q_4]^T$.

The dynamic model can be written:

$$M(q_c)\ddot{q} + h(q, \dot{q}) = \Gamma \tag{2}$$

where $M(q_c)$ is a (5×5) inertia matrix and vector $h(q, \dot{q})$ contains the centrifugal, Coriolis and gravity forces.

The fifth equation of system (1) is:

$$\frac{d}{dt}\left(\frac{\partial K}{\partial \dot{q}_5}\right) + \frac{\partial P}{\partial q_5} = \Gamma_a \tag{3}$$

For our planar biped and our choice of the coordinates in the single support, the term $\frac{\partial K}{\partial \dot{q}_5}$ is the angular momentum of the biped about the stance ankle A (Fig. 2). We denote this term by σ_A. Thus we have:

$$\frac{\partial K}{\partial \dot{q}_5} = \sigma_A = N(q_c)\dot{q} \tag{4}$$

where $N(q_c)$ is the fifth line of the inertia matrix $M(q_c)$.

The expression $\frac{\partial P}{\partial q_5}$ is equal to $-mgx_g$ if the abscissa of the stance ankle is 0, m is the mass of the biped, g is the gravity acceleration. Thus the fifth equation of the dynamic model of the biped in the single support can be written in the following simple form:

$$\dot{\sigma}_A - mgx_g = \Gamma_a \tag{5}$$

The Reaction Force During the Single Support Phase

The position of the mass center of the biped can be expressed as function of the angular coordinates vector q:

$$\begin{bmatrix} x_g \\ z_g \end{bmatrix} = \begin{bmatrix} f_{xi}(q) \\ f_{zi}(q) \end{bmatrix} \tag{6}$$

The vector-function $f_i(q) = [f_{xi}(q) \quad f_{zi}(q)]^T$ depends on vector q and on the biped parameters (lengths of the links, masses, positions of the centers of mass). The index i denotes the stance leg, for support on leg 1, $f_1(q)$ is used.

When leg 1 is on the ground, a ground reaction force, R_1, exists. The global equilibrium of the robot makes it possible to calculate this force:

$$m\begin{bmatrix}\ddot{x}_g\\ \ddot{z}_g\end{bmatrix}+mg\begin{bmatrix}0\\1\end{bmatrix}=R_1 \tag{7}$$

Equation (7) can also be written:

$$\begin{aligned} m\frac{\partial f_{x1}(q)}{\partial q}\ddot{q}+m\dot{q}^T\frac{\partial^2 f_{x1}(q)}{\partial q^2}\dot{q}=R_{x1}\\ m\frac{\partial f_{z1}(q)}{\partial q}\ddot{q}+m\dot{q}^T\frac{\partial^2 f_{z1}(q)}{\partial q^2}\dot{q}+mg=R_{z1}\end{aligned} \tag{8}$$

where $\frac{\partial^2 f_{x1}(q)}{\partial q^2}$ and $\frac{\partial^2 f_{z1}(q)}{\partial q^2}$ are (5×5) matrices.

Equilibrium of the Supporting Foot

The supporting foot is exposed to the ground reaction force and the ankle torque $-\Gamma_a$. The equilibrium law gives:

$$-\Gamma_a - lR_{z1} - h_pR_{x1} = 0 \tag{9}$$

Thus if the horizontal CoP position is l then the torque at the supporting ankle is, using (7):

$$\Gamma_a = -l(m\ddot{z}_g + mg) - h_p(m\ddot{x}_g) \tag{10}$$

The horizontal CoP position l is directly defined by the robot dynamics as it can be seen in the following equation obtained by combining equations (4), (5), (6), (8) and (10):

$$(N_0(q) + lN_l(q))\ddot{q} + h_0(q,\dot{q}) + lh_l(q,\dot{q}) = 0 \tag{11}$$

with

$$\begin{aligned} N_0 &= N(q_c) + mh_p\frac{\partial f_{x1}(q)}{\partial q}\\ N_l &= m\frac{\partial f_{z1}(q)}{\partial q}\\ h_0 &= \dot{q}^T\frac{\partial N(q_c)}{\partial q}\dot{q} - mgf_{x1}(q) + mh_p\dot{q}^T\frac{\partial^2 f_{x1}(q)}{\partial q^2}\dot{q}\\ h_l &= m\dot{q}^T\frac{\partial^2 f_{z1}(q)}{\partial q^2}\dot{q} + mg\end{aligned}$$

The Impact Model

When the swing leg 2 touches the ground with a flat foot at the end of the single support of leg 1, an inelastic impact takes place. We assume that the

ground reaction force at the instant of impact is described by a Dirac delta-function with intensity I_{R_2}. The velocity of foot 2 becomes zero just after the impact. Two kinds of impact can occur depending on whether the stance leg takes off or not. Here, for simplicity, we study walking with instantaneous double support. Thus at impact the stance leg 1 takes off and there is no impulsive ground reaction force on leg 1. The robot configuration q is assumed to be constant at the instant of impact, and there are jumps in the velocities. The velocity vectors just before and just after impact, are denoted $\dot{q}^-$ and $\dot{q}^+$ respectively. The torques are limited, thus they do not influence the instantaneous double support. It can be shown that the impact model can be written as [4]:

$$\dot{q}^+ = E(\triangle(q)\dot{q}^-) \tag{12}$$

where $\triangle(q)$ is a 5×5 matrix, and E is a permutation function describing the legs exchange. For the following single support phase the joints are relabelled in order to study only one dynamic model for single support (SS) and to take into account the change on the supporting ankle.

Intensity I_{R_2} of the impulsive reaction force is:

$$I_{R_2} = m\left(\frac{\partial f_2(q)}{\partial q}\triangle(q) - \frac{\partial f_1(q)}{\partial q}\right)\dot{q}^- \tag{13}$$

3 The First Control Law

In this study, walking is considered as single support phases with a full foot contact. While this is not a necessary condition for walking, and animals and humans do not enforce this constraint during walking, many control algorithms for bipedal robots enforce this constraint during walking in order to prevent difficulties associated with the loss of actuation authority when the foot rotates. To avoid foot rotation, the CoP must be inside the supporting area [13]. In order to ensure this behavior, the CoP position is controlled to follow a desired path l^d [11], but as shown in the previous section, the position of the CoP is directly connected to the dynamics of the motion. It is not possible to prescribe independently a desired evolution of the joints $q^d(t)$ and of the position of the CoP $l^d(t)$. With respect to such a task, the biped can be seen as an under-actuated system, and the control strategy developed for such a system can be used. Thus, the objective of the control law presented in this section is only to track a reference path for q and l rather than a reference motion [4]. A motion differs from a path by the fact that a motion is a temporal evolution along a path. A joint path is the projection of a joint motion in the joint space. The difference between motion and path are illustrated on Fig. 3 for a two joint-robot.

Only a geometrical tracking is desired and a time scaling control [6] is used. A reference joint path is assumed to be known. Thus the desired configuration of q and l for the biped are not expressed as a function of time. But they are

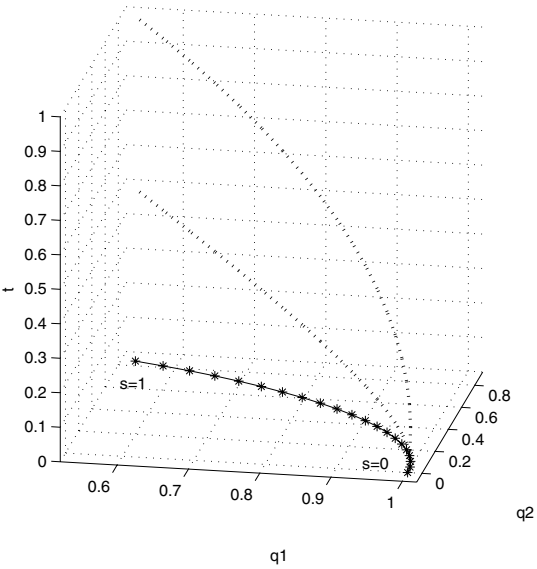

Fig. 3. The dotted lines are two motions $(q_1(t), q_2(t))$ corresponding to the same path represented by the solid line. A path is a line in the joint space, this line can be graduated as a function of a new variable denoted s, and then can be expressed by $(q_1(s), q_2(s))$. This function s is defined such that the initial configuration correspond to $s = 0$, the final configuration corresponds to $s = 1$. Any monotonic function $s(t)$ defines a motion corresponding to the path $q(s)$. For example $s = t/T$ defines a motion of duration T. If a joint variable, for example q_2, has a monotonic evolution along the path, the path can also be parametrized by q_2, in this case it can be expressed as $q_1(q_2)$

function of the scalar path parameter s, a normalized virtual time: $q^d(s), l^d(s)$. The desired walking of the robot corresponds to an increasing function $s(t)$. This function. $s(t)$ is not known a priori, the set of all the motions that correspond to the desired path is considered.

The proposed strategy can be extended without difficulty to walking including a rotation about the toe of the supporting foot, since this phase corresponds to a motion such that the position of the center of pressure is imposed. The main difficulty is that a sub-phase must be added [5].

3.1 Choice of a Reference Path

The reference path $q^d(s), l^d(s)$ is designed in order to obtain cyclic motion of the biped. The walk is composed of single supports separated by instantaneous passive impacts. The legs swap their roles from one step to the next one, so the reference path needs only to be defined for a single step. The evolution of the path parameter s along the step k is denoted $s_k(t)$, the scalar path

parameter s_k must increase strictly monotonically with respect to time from 0 to 1.

For $0 < s_k(t) < 1$, the robot configuration $q^d(s_k)$ is such that the swing leg is above the ground. The swing leg touches the ground at $s_k = 0, 1$ exactly. In consequence for any increasing function $s_k(t)$ from 0 to 1, the configuration of the biped at impact is the expected one. The control inputs are the torques. The torque acts on the second derivative of q and directly on l via the dynamic model. Thus the reference trajectory $q^d(s_k)$ must be twice differentiable, but no continuity condition exists for $l^d(s_k)$. Vectors $q^d(0)$ and $q^d(1)$ describe the initial and final biped configurations of the biped during a single support. As the legs swap their roles from one step to the following one the desired configurations are such that $q^d(1) = E(q^d(0))$ where E is a permutation function describing the leg exchange.

The reference path is defined such that if the reference path is exactly tracked before the impact then the reference path is exactly tracked after the impact. If the reference path is perfectly tracked, before the impact $k+1$, the vector of joint velocities is $\dot{q}^- = \frac{dq^d(1)}{ds}\dot{s}_k(1)$ and after the impact, $\dot{q}^+ = \frac{dq^d(0)}{ds}\dot{s}_{k+1}(0)$. The velocity at the end and at the beginning of the step are connected by the impact model and the legs exchange (12). Thus we have:

$$\frac{dq^d(0)}{ds}\dot{s}_{k+1}(0) = E(\triangle(q^d(1))\frac{dq^d(1)}{ds}\dot{s}_k(1)) \tag{14}$$

We choose:

$$\frac{dq^d(0)}{ds} = E(\triangle(q^d(1))\frac{dq^d(1)}{ds}\alpha) \tag{15}$$

With this choice we have the following equality: $\dot{s}_{k+1}(0) = \frac{\dot{s}_k(1)}{\alpha}$.

For configuration $q^d(1)$, and vector $\frac{dq^d(1)}{ds}$ the amplitude of the vector $\frac{dq^d(0)}{ds}$ can be modified by the choice the values of α (but not its direction). This point will be commented in Sect. 5.1.

Some hypotheses (no sliding, no rotation of the feet, take-off of the previous supporting leg) are made on the behavior of the robot at the impact, the corresponding constraints on the joint trajectory can be deduced [4, 7].

3.2 Definition of the Control Law

The control law must ensure that the joint coordinates follow the joint reference path $q^d(s)$ and that the position of the CoP is $l^d(s)$. It follows from the definition of the joints reference path that the desired velocity and acceleration of the joint variables are:

$$\begin{aligned} \dot{q}^d(t) &= \frac{dq^d(s(t))}{ds}\dot{s} \\ \ddot{q}^d(t) &= \frac{dq^d(s(t))}{ds}\ddot{s} + \frac{d^2q^d(s(t))}{ds^2}\dot{s}^2 \end{aligned} \tag{16}$$

The increasing function $s(t)$ defines the desired motion, but since the control objective is only to track a reference path, the evolution $s(t)$ is free and the second derivative $\ddot{s}$ will be treated as a "supplementary control input". Thus, the control law will be designed for a system with equal number of inputs and outputs. The control inputs are the five torques $\Gamma_j, j = 1, \ldots, 5$, plus $\ddot{s}$. The chosen outputs are the five angular variables of vector $q(t) - q^d(s(t))$ and $l(t) - l^d(s(t))$.

The control law is a non-linear control law classically used in robotics. But in order to obtain a finite-time stabilization of one of the desired trajectories, the feedback function proposed by Bhat and Berstein is used [1, 9]. The joint tracking errors are defined with respect to the trajectories satisfying (16):

$$\begin{aligned} e_q(t) &= q^d(s(t)) - q(t) \\ \dot{e}_q(t) &= \frac{dq^d(s(t))}{ds}\dot{s} - \dot{q}(t) \end{aligned} \tag{17}$$

The desired behavior in closed loop is:

$$\ddot{q} = \ddot{q}^d + \frac{1}{\epsilon^2}\psi \tag{18}$$

where ψ is a vector of five components $\psi_l, l = 1, \ldots, 5$ with:

$$\psi_l = -sign(\epsilon\dot{e}_{q_l})|\epsilon\dot{e}_{q_l}|^\nu - sign(\phi_l)|\phi_l|^\nu \tag{19}$$

and $0 < \nu < 1$, $\epsilon > 0$, $\phi_l = e_{q_l} + \frac{1}{2-\nu} sign(\epsilon\dot{e}_{q_l})|\epsilon\dot{e}_{q_l}|^{2-\nu}$, ν and ϵ are parameters to adjust the settling time of the controller. Taking into account the expression of the reference motion, (18) can be rewritten as:

$$\ddot{q} = \frac{dq^d(s)}{ds}\ddot{s} + v(s, \dot{s}, q, \dot{q}) \tag{20}$$

with

$$v(s, \dot{s}, q, \dot{q}) = \frac{d^2q^d(s)}{ds^2}\dot{s}^2 + \frac{1}{\epsilon^2}\psi$$

For the position of the CoP, the desired closed loop behavior is:

$$l(t) = l^d(s(t))$$

The dynamic model of the robot is described by eq. (2). The position of the CoP is defined via (11). Thus the control law must be such that:

$$\begin{aligned} M(q)(\frac{dq^d(s)}{ds}\ddot{s} + v) + h(q, \dot{q}) &= \Gamma \\ (N_0(q) + l^d(s)N_l(q))(\frac{dq^d(s)}{ds}\ddot{s} + v) + h_0(q, \dot{q}) + l^d(s)h_l(q, \dot{q}) &= 0 \end{aligned} \tag{21}$$

We can deduce that, in order to obtain the desired closed loop behavior, it is necessary and sufficient to choose:

$$\ddot{s} = \frac{-(N_0(q) + l^d(s)N_l(q))v - h_0(q,\dot{q}) - l^d(s)h_l(q,\dot{q})}{(N_0(q) + l^d(s)N_l(q))\frac{dq^d(s)}{ds}} \tag{22}$$

$$\Gamma = M(q)\left(\frac{dq^d(s)}{ds}\ddot{s} + v\right) + h(q,\dot{q}) \tag{23}$$

If $(N_0(q) + l^d(s)N_l(q))\frac{dq^d(s)}{ds} \neq 0$, the control law (22)–(23) ensures that $q(t)$ converges to $q^d(s(t))$ in a finite time, which can be chosen as less than the duration of one step [1, 9], and that $l(t) = l^d(s(t))$. Without initial errors, a perfect tracking of $q^d(s(t))$ and $l^d(s)$ is obtained.

3.3 Stability Study

Our main goal is to design a control strategy that ensures a stable periodic motion of the biped. The control law (22)–(23) ensures that the motion of the biped converges in a finite time toward a reference path. The settling time can be chosen to be less than the duration of the first step. Since the impact is a geometric condition and due to the characteristics of the joints reference path (Sect. 3.1), any step k begins with $s_k = 0$ and finishes with $s_k = 1$. Since the control law is designed to converge before the end of the first step and since the reference path is such that if the tracking is perfect before the impact, it will be perfect afterward, after the first step a perfect tracking is obtained. The biped with control law (22)–(23) follows perfectly the reference path, starting from the second step. Thus:

$$\begin{aligned} q(t) &= q^d(s(t)) \\ \dot{q}(t) &= \frac{dq^d(s)}{ds}\dot{s}(t) \\ \ddot{q}(t) &= \frac{dq^d(s)}{ds}\ddot{s}(t) + \frac{d^2q^d(s)}{ds^2}\dot{s}(t)^2 \\ l(t) &= l^d(s(t)) \end{aligned} \tag{24}$$

These equations define the zero dynamics corresponding to the proposed control law. To know whether a cyclic motion will be obtained, the behavior of the evolution of $\dot{s}_k(t)$ is studied for $k = 2 \ldots \infty$. The dynamics of s is deduced from the dynamic model (11) with the condition (24). The acceleration $\ddot{s}$ is:

$$(N_{s0}(s) + l^d(s)N_{sl}(s))\ddot{s} + h_{s0}(s,\dot{s}) + l^d(s)h_{sl}(s,\dot{s}) = 0 \tag{25}$$

with

$$
\begin{aligned}
N_{s0} &= (N(q^d(s)) + mh_p \frac{\partial f_{x1}(q)}{\partial q}) \frac{dq^d(s)}{ds} \\
N_{sl} &= m \frac{\partial f_{z1}(q)}{\partial q} \frac{dq^d(s)}{ds} \\
h_{s0} &= \left[\frac{dq^d(s)}{ds}^T \left(\frac{\partial N(q)}{\partial q} + mh_p \frac{\partial^2 f_{x1}(q)}{\partial q^2} \right) \frac{dq^d(s)}{ds} \right] \dot{s}^2 \\
&\quad + \left[\left(N(q^d(s)) + mh_p \frac{\partial f_{x1}(q)}{\partial q} \right) \frac{d^2 q^d(s)}{ds^2} \right] \dot{s}^2 \\
&\quad - mg f_{x1}(q^d(s)) \\
h_{sl} &= m \left[\frac{dq^d(s)}{ds}^T \frac{\partial^2 f_{z1}(q)}{\partial q^2} \frac{dq}{ds} + \frac{\partial f_{z1}(q)}{\partial q} \frac{d^2 q^d(s)}{ds^2} \right] \dot{s}^2 + mg
\end{aligned}
\tag{26}
$$

This equation along with the constraints (24) describe completely the behavior of the system.

One single support phase begins with $s = 0$ and finishes with $s = 1$. The evolution of $\dot{s}_{k+1}$ during the step $k + 1$ is uniquely defined by initial value $\dot{s}_{k+1}(0)$. The integration of (25) along one step, starting with $\dot{s}_{k+1}(0)$, defines the final value $\dot{s}_{k+1}(1)$.

The single support phases are separated by impact phases; the evolution of the zero dynamics is such that s restarts with $s = 0$ and $\dot{s}_{k+1}(0) = \frac{\dot{s}_k(1)}{\alpha}$ (due to the definition of the reference joint path (15)). Thus the final value of $\dot{s}_{k+1}(1)$ can be easily defined numerically as a function of $\dot{s}_k(1)$, we define function φ by: $\dot{s}_{k+1}(1) = \varphi(\dot{s}_k(1))$. The existence of a cyclic motion and the convergence to it can be studied via function φ as it is classically done using the method introduced by H. Poincaré [9, 10]. The fixed point of this function defines the cyclic velocity $\dot{s}_c(1)$, it corresponds to the intersection between the function φ and the identity function. If the norm Δ of the slope of the function φ at $\dot{s}_c(1)$ is less than 1, then for an initial state close to the cyclic motion, the biped motion will converge toward the cyclic motion.

If the desired evolution of the position of the CoP is piecewise constant, the stability analysis can be conducted mostly analytically [7]. If the desired evolution of the position of the CoP is arbitrary, the stability analysis is conducted numerically in this chapter.

4 The Second Control Law

The physical constraint on the position of the CoP is that the position of the CoP is between l_{min} and l_{max} but it is not necessary that $l(s)$ follows exactly $l^d(s)$. If a cyclic motion corresponding to $q^d(s)$, $l^d(s)$ exists, it can be interesting to converge quickly toward this cyclic motion defined by $\dot{s}(t) = \dot{s}_c(t)$. The corresponding cyclic motion can be defined by the stability study

of the first control law. Now we assume that the corresponding cyclic motion is given as a function $\dot{s}_c(s)$ for $0 \leq s \leq 1$. To achieve this objective, the constraint $l(s) = l^d(s)$ can be relaxed to: $l_{min} < l(s) < l_{max}$.

To converge toward the cyclic orbit in the phase plane $s, \dot{s}$, we define an error between the current state and the orbit:

$$e_v = \dot{s}(s) - \dot{s}_c(s) \tag{27}$$

and to nullify this error the desired acceleration $\ddot{s}^d$ is chosen such that: $\dot{e}_v + K_{vs} e_v = 0$ where K_{vs} defines the convergence rate to the cyclic motion. Thus the desired acceleration is:

$$\ddot{s}(s)^d = \frac{d(\dot{s}_c(s))}{ds}\dot{s} + K_{vs}(\dot{s}_c(s) - \dot{s}(s)) \tag{28}$$

But the position l of the CoP, and the acceleration $\ddot{s}$ are linked by the dynamic model. And even if the constraint on l is relaxed, the condition of non-rotation of the feet holds, and l is monitored to be within the domain $\Im =]l_{min}, l_{max}[$ in all the control process. If the same closed loop behavior is desired for the joint variables (22), gives:

$$\ddot{s} = \frac{-N_0(q)v - h_0(q,\dot{q}) + l(N_l(q)v - h_l(q,\dot{q}))}{N_0(q)\frac{dq^d(s)}{ds} + lN_l(q)\frac{dq^d(s)}{ds}} \tag{29}$$

where l must be chosen such that $l \in \Im$. Differentiating (29) with respect to l shows that $\ddot{s}$ is monotonic with respect to l. Thus the limits $l_{min} < l < l_{max}$ can be easily transformed with limits on $\ddot{s}$. For this purpose, the extreme values for $\ddot{s}$ are defined as follows:

$$\begin{aligned} u_1 &= \frac{-N_0(q)v - h_0(q,\dot{q}) + l_{min}(N_l(q)v - h_l(q,\dot{q}))}{N_0(q)\frac{dq^d(s)}{ds} + l_{min}N_l(q)\frac{dq^d(s)}{ds}} \\ u_2 &= \frac{-N_0(q)v - h_0(q,\dot{q}) + l_{max}(N_l(q)v - h_l(q,\dot{q}))}{N_0(q)\frac{dq^d(s)}{ds} + l_{max}N_l(q)\frac{dq^d(s)}{ds}} \end{aligned} \tag{30}$$

For given values of s, $\dot{s}$, two cases occur depending on whether the denominator can be zero or not for $l \in \Im$. The denominator is zero for $l(s) = -\frac{N_0(q)\frac{dq^d(s)}{ds}}{N_l(q)\frac{dq^d(s)}{ds}}$. If for any l such that $l \in \Im$, the denominator of eq. (29) is not zero, then $\ddot{s}$ is bounded for any acceptable value l and $\min(u_1, u_2) < \ddot{s} < \max(u_1, u_2)$. If for one value l such that $l \in \Im$, the denominator of eq. (29) is zero, then $\ddot{s}$ is unbounded and $\ddot{s}$ cannot be in the interval $]\min(u_1, u_2), \max(u_1, u_2)[$ with acceptable values of l.

Thus the proposed control law is the following: like the previous control law, the reference path $q^d(s)$ is tracked using eq. (23) but eq. (22), which corresponds to the constraint $l(s) = l^d(s)$, is replaced by the following:

$$
\begin{aligned}
&\text{if } -\frac{N_0(q)\frac{dq^d(s)}{ds}}{N_l(q)\frac{dq^d(s)}{ds}} < l_{min} \text{ or } -\frac{N_0(q)\frac{dq^d(s)}{ds}}{N_l(q)\frac{dq^d(s)}{ds}} > l_{max} \text{ then}\\
&\qquad \ddot{s} = \begin{cases} \min(u_1,u_2), & \text{if } \ddot{s}^d < \min(u_1,u_2) \\ \max(u_1,u_2), & \text{if } \ddot{s}^d > \max(u_1,u_2) \\ \ddot{s}^d, & \text{otherwise} \end{cases}\\
&\text{if } l_{min} < -\frac{N_0(q)\frac{dq^d(s)}{ds}}{N_l(q)\frac{dq^d(s)}{ds}} < l_{max} \text{ then}\\
&\qquad \ddot{s} = \begin{cases} \min(u_1,u_2), & \text{if } \min(u_1,u_2) < \ddot{s}^d \le u_{12} \\ \max(u_1,u_2), & \text{if } u_{12} < \ddot{s}^d < \max(u_1,u_2) \\ \ddot{s}^d, & \text{otherwise} \end{cases}
\end{aligned}
\tag{31}
$$

where $u_{12} = \frac{\min(u_1,u_2)+\max(u_1,u_2)}{2}$. This control law ensures a convergence to the cyclic motion with a convergence rate defined by K_{vs} under the constraint $l \in \Im$.

The control law (31), (23) ensures that $q(t)$ converges to $q^d(s(t))$ in a finite time, which can be chosen less than the duration of one step [1, 9], and ensures that $l \in \Im$. The biped with control law (31), (23) follows perfectly the reference path after this first step. To know if a cyclic motion will be obtained, the behavior of the evolution of $\dot{s}_k(t)$ is studied for $k = 2 \ldots \infty$ and for an initial velocity $\dot{s}_2(0)$. The stability analysis is done numerically like for the first control law.

The convergence rate to the cyclic motion depends on the choice of the value K_{vs}. Higher values of K_{vs} speed up convergence toward the cyclic motion if there is no saturation due to the limits on l.

5 Walking Simulation using Correct Model Parameters

5.1 A Reference Path

The proposed control law was tested on the reference path corresponding to the stick-diagram presented in Fig. 4, for the biped presented in Fig. 1. The joint path $q^d(s)$ is defined by a fourth order polynomial evolution with respect to s.

This reference path has been defined to produce an optimal cyclic motion for the robot Rabbit [2], this robot has the same physical property that the robot described in Sect. 2 but Rabbit has no feet ($h_p = 0$, $l = 0$). As the studied robot has feet, and a linear evolution of the position of the CoP is considered, the existence of a cyclic motion is not ensured and if it exists it is of course not optimal.

For the robot without feet, the optimization process is described in [8]. The reference path is described by an instantaneous double support configuration

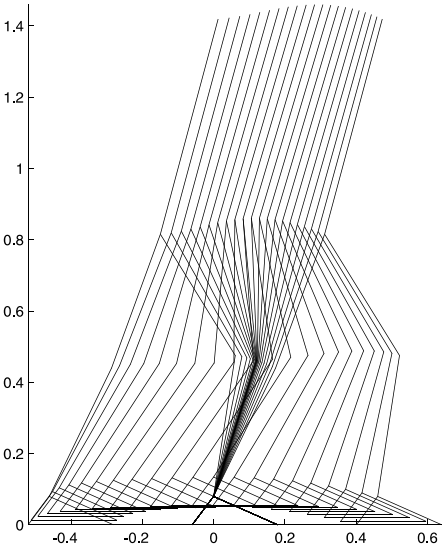

Fig. 4. The stick diagram of the desired trajectory. The configuration of the robot are drawn for $s = 0, 0.05, 0.1, 0.15 \ldots, 0.95, 1$. Thus a sequence of pictures of the robot are given. The desired motions of the robot are such that the configuration of the robot coincides at some instant to each picture, but it is not imposed that these instants are equally distributed in the period of one step

$q^d(1)$, the final direction of the joint velocity $\frac{q^d(1)}{ds}$, an intermediate single support configuration $q^d(0.5)$, and α. The initial double support configuration is defined by permutation: $q^d(0) = Eq^d(1)$. The direction of the initial velocity is defined by equation (15). Then the desired path is determined by a polynomial 4th order function of s connecting these configurations and velocities. The integral of the norm of the torque for the cyclic motion is minimized for a given advance velocity. The free leg tip must be above a sinusoidal function with a maximum of 5 cm. The limit of the actuator are taken into account (maximal torque less than 150 Nm). The reference path corresponding to the Fig. (4) is obtained for given advance velocity $vel = 1.41\,\mathrm{ms}^{-1}$. The optimal solution is such that: $q^d(1) = [5.73^\circ\ 185.08^\circ\ 40.43^\circ\ 133.33^\circ\ 25.81^\circ]^T$, $\frac{q^d(1)}{ds} = [3.57^\circ s^{-1}\ 32.60^\circ s^{-1}\ -61.60^\circ s^{-1}\ 0.09^\circ s^{-1}\ 29.50^\circ s^{-1}]^T$, $q^d(0.5) = [19.97^\circ\ 161.22^\circ\ 42.51^\circ\ 154.93^\circ\ 17.72^\circ]^T$ and $\alpha = 1.98$

5.2 The First Control Law

For this joints path, a linear evolution of the CoP position is chosen. When s varies from 0 to 1, l^d varies from $-0.06\,\mathrm{m}$ to $0.18\,\mathrm{m}$.

The control law imposes that $q(s) = q^d(s)$, $l(s) = l^d(s)$ after the first step. The stability of the complete system is determined by the evolution of $s(t)$. It

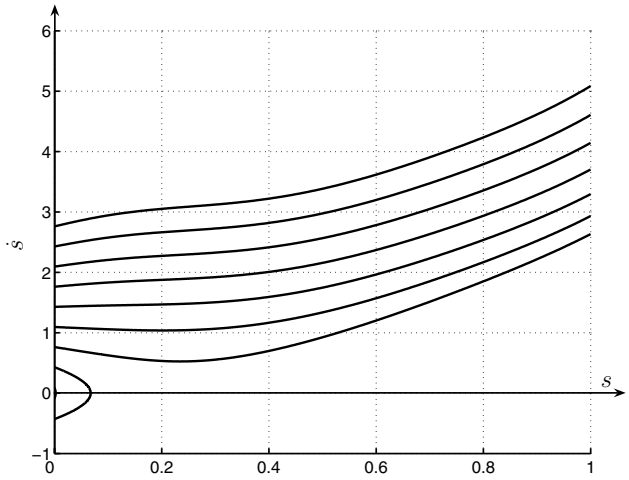

Fig. 5. The phase plane for the zero dynamics (25) on single support: $\dot{s}$ against s

can be described in a phase plane $s, \dot{s}$ for $0 \leq s \leq 1$ initialized with different values for $\dot{s}$. For example, the phase plane is shown in Fig. 5.

For a sufficiently high initial velocity $\dot{s}(0)$, successful stepping pattern can be achieved. At low initial velocity $\dot{s}(0)$, the robot falls back. Taking the impact phase into account (here $\alpha = 1.98$), the Poincaré return map $\dot{s}_{k+1}(1) = \varphi(\dot{s}_k(1))$ is drawn in Fig. 6. For the example the cyclic motion is such that $\dot{s}_c(1) = 3.9\,\mathrm{s}^{-1}$. The corresponding average motion velocity is $vel = 1.5$ m/s. The slope of function φ is estimated numerically: $\Delta = 0.68$; it is less than 1, thus the proposed control law is stable. The minimal value and the maximal value of the velocity $\dot{s}_k(1)$ such that the step can be achieved are defined numerically. For smaller initial velocities the biped falls back, for higher velocities the biped takes off since the normal ground reaction vanishes.

Assuming no modeling error and initializing the state of the biped out of the periodic orbit (with an initial velocity 60% higher than the cyclic value), the results of one simulation for 20 walking steps are illustrated in Fig. 7. The convergence toward a cyclic motion can be shown for the five joints via their evolution in their phase plane. For example the evolution of the trunk is shown in Fig. 7-a. This convergence is also illustrated via the evolution of the position of the CoP with respect to time in Fig. 7-b. For each step, this evolution is linear from -0.06 m to 0.18 m, but the duration of the step varies. At the beginning;, the steps are faster and then a cyclic behavior is obtained. Figure 7-c presents the time-history of $\dot{s}$, it clearly converges toward a cyclic motion, the final value of $\dot{s}$ before each impact is the cyclic value obtained on the Poincaré map.

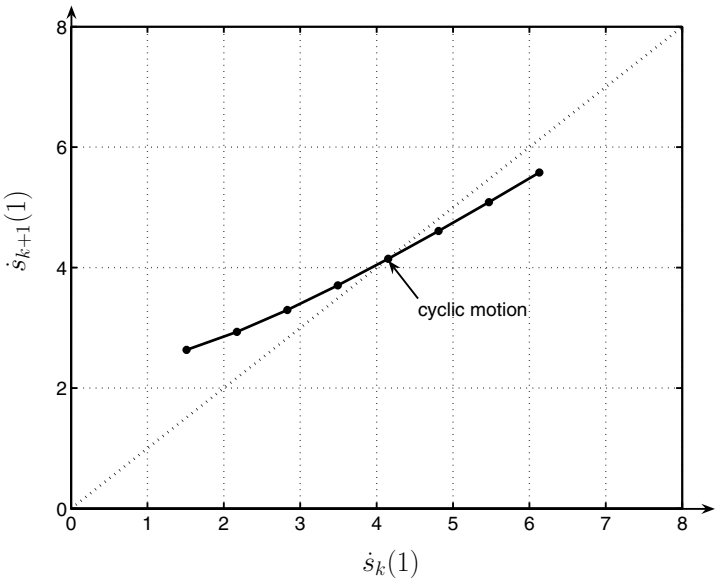

Fig. 6. The Poincaré map: $\dot{s}_{k+1}(1) = \varphi(\dot{s}_k(1))$

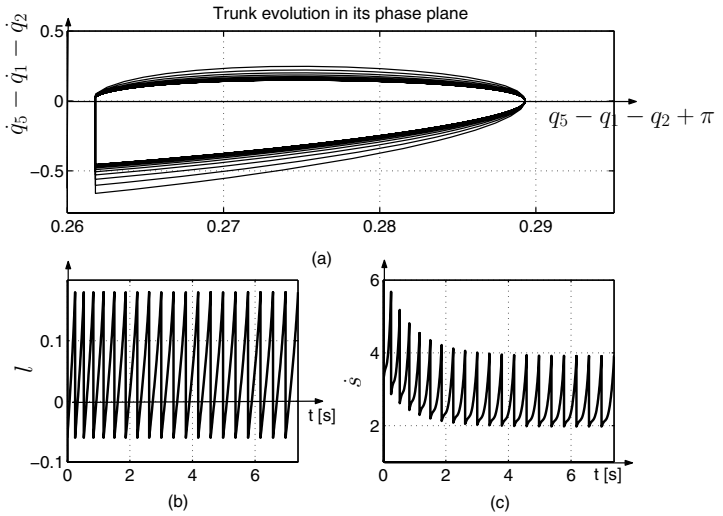

Fig. 7. The convergence toward a cyclic motion is observed in simulation with the proposed control law, without modeling error. (**a**) The trunk evolution is drawn in its phase phase (the absolute trunk velocity with respect to the absolute trunk orientation), at impact the velocity changes but not the orientation. It tends toward a limit cycle. (**b**) During each step, the *horizontal* position of the CoP with respect to time $l(t)$ evolves from $-0.06\,\mathrm{m}$ to $0.18\,\mathrm{m}$. The duration of the step tends toward a constant value. (**c**) $\dot{s}(t)$ tends toward a cyclic motion

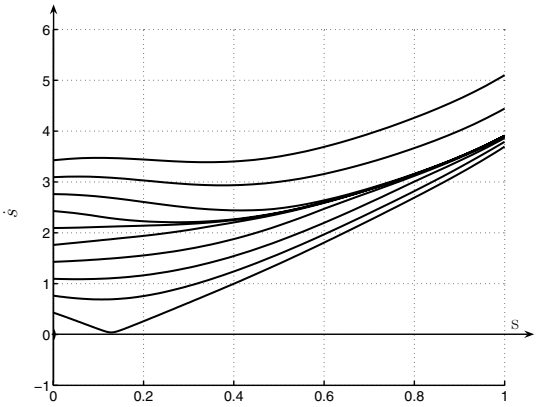

Fig. 8. The phase plane for the zero dynamics on single support, (31), for the second control law with $K_{vs} = 20$

5.3 The Second Control Law

The second control law was tested on the same reference trajectory $q^d(s)$. The desired evolution of $\dot{s}(s)$ is the cyclic motion corresponding to the previous control law.

The control law imposes some constraints $q(s) = q^d(s)$ that are assumed to be perfectly respected. The free dynamics that results from imposing these constraints on the system configuration are described by $s, \dot{s}$ and eq. (31) can be represented in the phase plane. The phase plane is shown in Fig. 8 for $K_{vs} = 20$.

The convergence toward the cyclic motion is clear when Figs. 5 and 8 are compared. When $K_{vs} = 20$, for initial velocities varying from 1.4 to 2.8, the cyclic motion is reached in one step. This feature gives a horizontal behavior of the Poincaré map about the fixed point. The motion can be initiated with a lower velocity $\dot{s}(0)$ than for the first control law because when the current motion converges toward the cyclic motion, it helps prevent the biped from falling back.

The control strategy is properly illustrated by the evolution of $l(s)$ corresponding to the evolution of the biped for various initial velocities $\dot{s}(0)$ in Fig. 9. When the real motion of the biped is slower than the cyclic one, the position of the CoP is moved backwards to increase the motion velocity until the limit l_{min} is reached. When the real motion of the biped is faster than the cyclic one, the position of the CoP is moved forwards to decrease the motion velocity until the limit l_{max} is reached. With a high gain, the position of the CoP is on the limit almost all the time

The single support phases are separated by impact phases. The Poincaré return maps can be deduced and are presented in the Fig. 10, for $K_{vs} = 2$ and $K_{vs} = 20$.

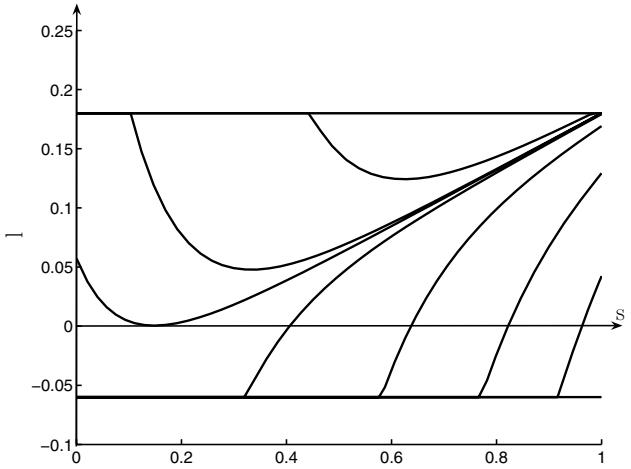

Fig. 9. The evolution of the position of the CoP $l(s)$, for various initial velocities $\dot{s}(0)$, for the second control law with $K_{vs} = 20$

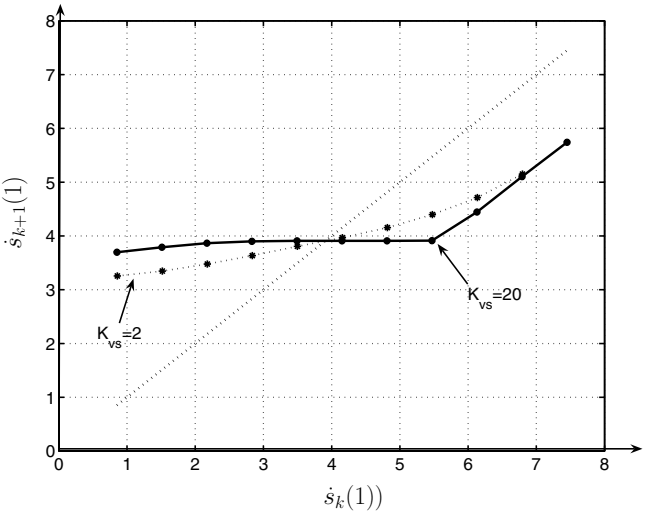

Fig. 10. The Poincaré return map for the second control law with $K_{vs} = 2$ (*solid line*) and $K_{vs} = 20$ (*dotted line*), $\dot{s}_{k+1}(1)$ is shown against $\dot{s}_k(1))$

Since this control law is defined to obtain convergence toward the cyclic motion corresponding to the first control law, the fixed point of the Poincaré maps is the same (see Figs. 6, 10). The minimal and maximal values of the velocity $\dot{s}_k(1)$ such that the step can be achieved are defined numerically. It can be noted that the minimal initial velocity is lower for the second control strategy than for the first one. With $K_{vs} = 2$, at the fixed point the slope is

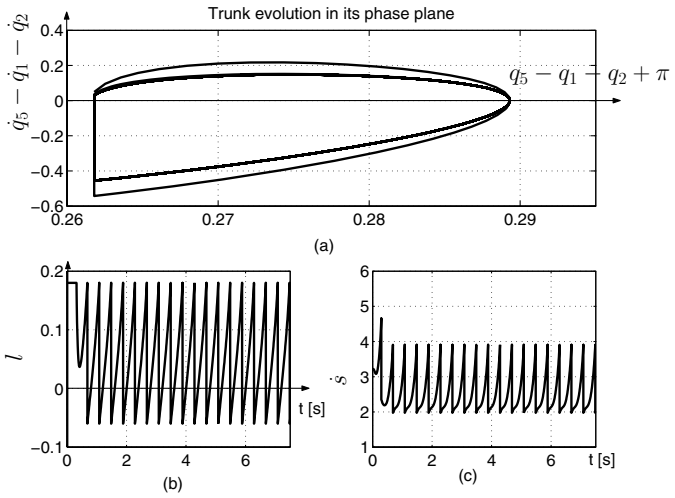

Fig. 11. The convergence toward a cyclic motion is observed in simulation with the second control law, with $K_{vs} = 20$, without modeling error. (**a**) The trunk evolution is drawn in its phase phase (the absolute trunk velocity with respect to the absolute trunk orientation), it tends toward a limit cycle. (**b**) The *horizontal* position of the CoP with respect to time $l(t)$ is bounded. It tends toward the same cyclic evolution as in Fig. 7(b). (**c**) $\dot{s}(s)$ tends toward to the same cyclic motion as in Fig. 7(c)

about $\Delta = 0.23$; it is less than the value obtained for the first control law thus the convergence is faster. For $K_{vs} = 20$ the convergence is so fast that the slope is close to horizontal at the fixed point, in one step the cyclic motion is almost joined. When the initial velocity is far beyond the cyclic one, the constraint on l produces a saturation on $\ddot{s}$ almost all the time, thus almost the same behavior is obtained with $K_{vs} = 2$ or $K_{vs} = 20$.

Assuming no modeling error and initializing the state of the robot out of the periodic orbit (with an initial velocity 60% higher than the cyclic value), the results of one simulation for 20 walking steps of the robot are illustrated in Fig. 11. The convergence toward a cyclic motion can be shown for the trunk via its evolution in its phase plane (Fig. 11-a). In one step the cyclic motion is reached. This convergence is also illustrated via the evolution of the position of the CoP with respect to time (Fig. 11-b). To slow down the motion, for the first step, the position of the CoP stays on the front limit (l_{max}). After the evolution of the CoP corresponds to the desired cyclic one, it is linear from $-0.06\,\mathrm{m}$ to $0.18\,\mathrm{m}$. Figure 11-c presents the evolution of $\dot{s}$ with respect to time, it clearly converges toward the desired cyclic motion.

6 Control of Walking with Imprecise Model Data

In practice the robot parameters are not perfectly known. We assume that we have some errors on the masses and consequently on the inertia moments of the robot links. We simulate the following case of errors:

- the mass errors are: +10% for the thighs, +30% for the shanks and +50% for the trunk. The error on the inertia moment of the trunk is +30%;
- since the reference path is designed with a false model, the velocity after the impact is not the expected one;
- as the position l of the CoP is calculated via the dynamic model, $l(s)$ will not be exactly $l^d(s)$.

This choice of errors is arbitrary. We choose that the real robot is heavier than the model used in the control law, this point is commented.

6.1 The First Control Law

Initializing the state of the robot in the same conditions as in 5.2; the behavior obtained for 20 walking steps is presented in Fig. 12. Some tracking errors exist particularly at the beginning of each step due to the effect of impact, thus the path followed is not exactly the expected one (but the tracking errors

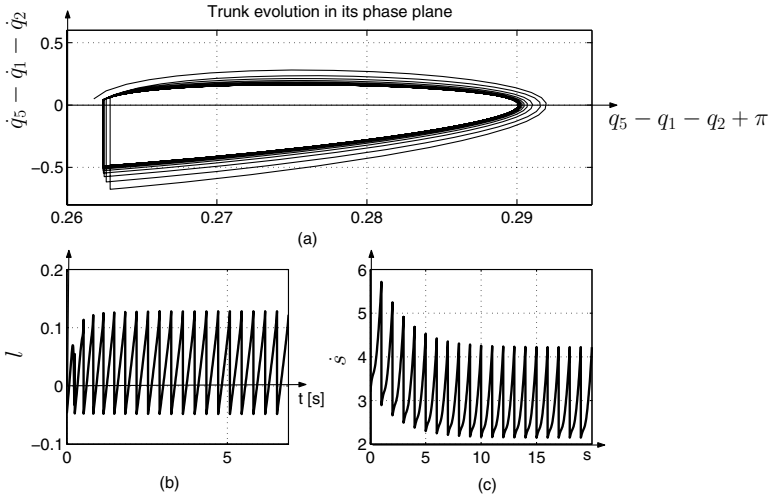

Fig. 12. The convergence toward a cyclic motion is observed in simulation with the proposed control law, with modeling error. (**a**) The trunk evolution is drawn in its phase phase (the absolute trunk velocity with respect to the absolute trunk orientation), it tends toward a limit cycle. (**b**) The *horizontal* position of the CoP with respect to time $l(t)$ tends toward a cyclic evolution different from Fig. 11(b). (**c**) $\dot{s}(s)$ tends toward a cyclic motion different from the motion in Fig. 7(c)

are cyclic). The convergence toward a cyclic motion is shown for the trunk evolution via its phase plane in Fig. 12-a. This convergence is also illustrated via the evolution of $\dot{s}$ with respect to s in Fig. 12-c, it clearly converges toward a stable cyclic motion. The cyclic motion is close to the expected one but not exactly the same, because it is the result of the motion of the CoP and of the dynamic model. Since the real robot is heavier than the robot's model used, we have greater ground reaction forces; consequently the real evolution l of the CoP in Fig. 12-b varies between extreme values smaller in absolute value than the desired values. The difference between $l(s)$ and $l^d(s)$ is higher for large value of $\dot{s}$. In this case there is no problem because constraints of equilibrium of the supporting foot are always satisfied. Otherwise if the real robot was lighter than the modeled one, the CoP could be outside the sole and the constraints of equilibrium of the supporting foot could be violated. So a security margin is necessary when the minimum and the maximum values for the CoP evolution are defined. The best way is to define l_{min} and l_{max} with some margins with respect to real size of the foot (see Fig. 2).

6.2 The Second Control Law

In order to illustrate some robustness properties of the second control law proposed in (Sect. 4), we test the same modeling error as in Sect. 6.

- Since the reference path is designed with a false model, the velocity after the impact is not the expected one;
- In the case of perfect modeling the control law (31) assumes that the limits on $\ddot{s}$ corresponds to $l_{min} < l < l_{max}$. But this relation is based on the dynamic model, since the dynamic model is not perfectly known, this transformation will induce some errors.

A simulation of 20 walking steps is presented in Fig. 13. The biped state is initialized out of the periodic orbit (with an initial velocity 60% higher than the cyclic value). The convergence toward a cyclic motion can be shown via the trunk evolution in its phase plane in Fig. 13-a; some errors can be observed at the impact times. The convergence toward the cyclic motion can be also shown in Fig. 13-b via the evolution of the CoP with respect to time. The evolution of the CoP is not the expected one even if the evolution of $\dot{s}$ converges clearly toward the expected cyclic motion with the end of the second step (Fig. 13-c and 12-c).

In the presence of modeling errors, the two control laws will not give the same cyclic behavior. Due to the second control law, $\dot{s}$ will converge toward $\dot{s}_c$, and the average velocity of the robot does not change, which is not the case for the first control law.

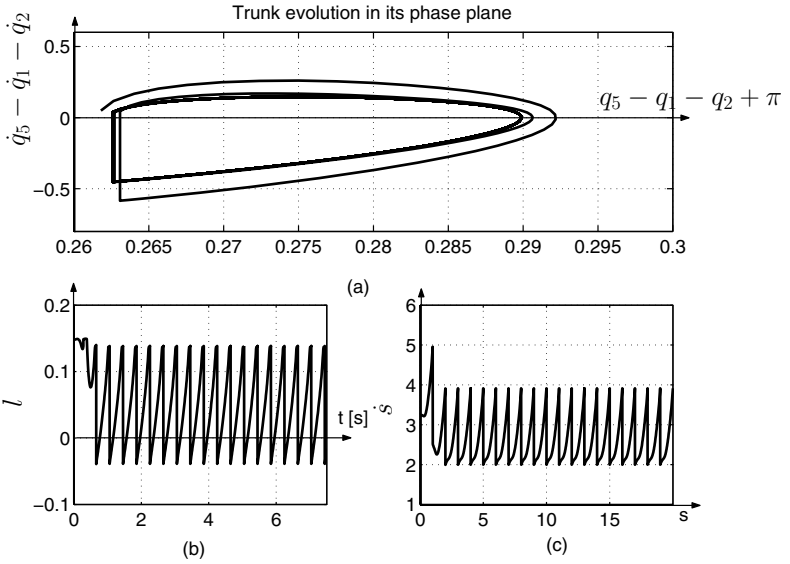

Fig. 13. The convergence toward a cyclic motion is observed in simulation with the second control law, with K_{vs}=20, with modeling errors. (**a**) The trunk evolution is drawn in its phase phase (the absolute trunk velocity with respect to the absolute trunk orientation), it tends toward a limit cycle. (**b**) The horizontal position of the CoP with respect to time $l(t)$ is bounded. It tends toward a cyclic evolution different from Fig. 11(b). (**c**) $\dot{s}(s)$ tends toward to the same cyclic motion as in Fig. 7(c)

7 Discussion Section

Even if the stability studies for the two proposed control laws are conducted numerically for the examples, based on the analytical study of the robot without feet [4] and on the case of a desired piecewise evolution of the position of the center of pressure [7], and also based on numerous simulations, some general conclusions can be given:

- For the first control law, the choice of $l^d(s)$ has a large effect on the existence of a cyclic motion and on the average velocity of the robot. If the position of the CoP is moved forward, the average velocity of the cyclic motion is slowed down. This property is limited: if the position of the CoP is too much forward, no cyclic motion exists. In order that the robot walks faster, a simple solution is to move the desired evolution of the CoP backward.
- The stability property of the first control strategy is essentially due to the fact that the vertical velocity of the center of mass is directed downward just before the impact [4], [7]. Thus this property depends essentially on the choice of $q^d(s)$.

- A larger variation of $l^d(s)$ during one step has two effects, the basin of attraction of the control law is slightly increased, the convergence rate is slightly decreased.
- For the first control law, the control speed $\dot{s}$ is not directly controlled, as shown in Fig. 5, but only stabilizes step by step. The impact phase has a key role in this stabilization. For the example, if the single support phase can be achieved, $\dot{s}$ increases non linearly during the single support and decreases linearly during the impact phase, thus a stable speed is reached as in a passive walking.
- When the desired joint references and the desired position of the center of pressure are defined, since they are not function of time, we do not have to worry about the dynamic consistency. The joints reference need only to be twice differentiable and to satisfy the start and stop conditions corresponding to the impact model. The second derivative of s is calculated to satisfy the dynamic consistency.
- In the development of the control, a finite time controller is defined in eq. (18), to insure a fast convergence to the zero dynamic manifold. Such a controller is not required for the simulation and experiments. The dynamic model is used to calculate the position of the CoP and the admissible limits, for the experiments because it implies that the dynamic model must be "correctly" known. The robustness tests (Sect. 6) have demonstrated that an acceptable behavior can be obtained in the presence of an imprecise model.
- For the second control law, an arbitrary function $\dot{s}_c(s)$ can be chosen even if $\frac{\dot{s}_c(1)}{\dot{s}_c(0)} \neq \alpha$. If this function $\dot{s}_c(s)$ is not consistent with the constraint on the dynamic model ($l_{min} < l(s) < l_{max}$), the closed loop system will converge to an evolution "close" to $\dot{s}_c(s)$ but consistent with the constraint on the dynamic model. This can be used to choose faster or slower motion. For the proposed example, if we choose $\dot{s}_c = 1$, we obtain a cyclic motion with an average velocity of $0.51\,\mathrm{ms}^{-1}$, the CoP position is in the forward part of the feet and often on the toe limit. If we choose $\dot{s}_c = 4$ we obtain a cyclic motion with an average velocity of $1.5\,\mathrm{ms}^{-1}$, the CoP position is often in the limit of the foot.
- The proposed control laws can be extended to walking including rotation of the foot about the toe [5].
- We hope that the second control strategy can be directly used for robot walking in 3D, even if the position of the CoP is limited in the sagittal and frontal plane.

8 Conclusion

For a planar biped, the proposed control strategy consists in the tracking of a reference path instead of a reference motion for the joints and for the position of the CoP. The biped adapts its temporal evolution according to the dynamic

constraint that relies the position of the CoP and the joint acceleration. In this context a complete study has been presented.

The conditions of stability are inequalities. Thus a certain robustness is naturally contained in the proposed control strategy. In spite of tracking errors and/or modeling errors, the behavior of the biped converges to a cyclic motion. In the presence of modeling errors, the obtained cycle is slightly modified with respect to the predicted cycle, but stable walking is obtained as it has been observed in simulation.

Two control strategies have been proposed. In the first case, the CoP is constrained to be a function of the robot configuration and the geometric evolution of the joints are controlled, but the temporal evolution is free; the natural convergence toward a cyclic motion is used. In the second case, the convergence to the cyclic motion is forced by using the CoP as a control input to correct for errors in the configuration speed, $\dot{s}$, and the limits on the CoP position are used $l_{min} < l < l_{max}$.

References

[1] S. P. Bhat and D. S. Bernstein. Continuous finite-time stabilization of the translational and rotational double integrators. *IEEE Transaction on Automatic Control*, 43(5):678–682, 1998.

[2] C. Chevallereau, G. Abba, Y. Aoustin, F. Plestan, E. R. Westervelt, C. Canudas-de Witt, and J. W. Grizzle. Rabbit: A testbed for advanced control theory. *IEEE Control System Magazine*, 23(5):57–78, 2003.

[3] C. Chevallereau and A. Lounis. On line reference trajectory adaptation for the control of a planar biped. In *5th international Conference on Climbing and Walking Robots CLAWAR*, pp. 427–435, Paris, France, 2002.

[4] C. Chevallereau, Formal'sky A. M., and D. Djoudi. Tracking of a joint path for the walking of an under actuated biped. *Robotica*, 22(1):15–28, 2004.

[5] Jun Ho Choi and J.W. Grizzle. Planar bipedal walking with foot rotation. In *paper submitted to ACC*, 2005.

[6] O. Dahl and L. Nielsen. Torque-limited path following by online trajectory time scaling. *IEEE Trans. on Automat. Contr*, 6(5):554–561, 1990.

[7] D. Djoudi and C. Chevallereau. Stability analysis of a walk of a biped with control of the zmp. In *IROS'05*, 2005.

[8] D. Djoudi, C. Chevallereau, and Y. Aoustin. Optimal reference motions for walking of a biped robot. In *ICRA 05*, 2005.

[9] J. W. Grizzle, G. Abba, and F. Plestan. Asymptotically stable walking for biped robots: analysis via systems with impulse effects. *IEEE Trans. on Automat. Contr.*, 46:51–64, 2001.

[10] J. Guckenheimer and P. Holmes. *Nonlinear Oscillations, Dynamical Systems, and Bifurcations of Vector Fields*. Springer-Verlag, 1985.

[11] K. Hirai, M. Hirose, Y. Haikawa, and T. Takenaka. The development of honda humanoï¿½ robot. In *Proc. of the IEEE International Conference on Robotics and Automation*, pp. 1321–1326, Leuven, Belgium, 1998.

[12] F. Pfeiffer, K. Loffler, and M. Gienger. The concept of jogging johnie. In *IEEE Int. Conf. on Robotics and Automation*, 2002.

[13] M. Vukobratovic and B. Borovac. Zero moment point -thirty five years of its live. *Int. Journal of Humanoid Robotics*, 1(1):157–173, 2004.

[14] M. Vukobratovic, B. Borovac, D. Surla, and D. Stokic. *Biped Locomotion*. Springer-Verlag, 349p, 1990.

[15] E.R. Westervelt, J.W. Grizzle, and D.E. Koditschek. Hybrid zero dynamics of planar biped walkers. *IEEE Transaction on Automatic Control*, 48(1):42–56, 2003.

[16] P.-B. Wieber and C. Chevallereau. Online adaptation of reference trajectories for the control of walking systems. *Robotics and Autonomous Systems*, 54:559–566, 2006.